Avrupa Bilim ve Teknoloji Dergisi
Özel Sayı 36, S. 134-138, Mayıs 2022

Araştırma Makalesi

www.ejosat.com ISSN:2148-2683

European Journal of Science and Technology
Special Issue 36, pp. 134-138, May 2022

Research Article

Dual-band Band-pass Tunable Filter with Meander-Line Resonator

Mert Demirel[1*]

[1*] Izmir Katip Celebi University, Faculty of Engineering and Architecture, Departmant of Electrical and Electronics Engineering, Izmir, Turkey, (ORCID: 0000-0001-7905-8456), mdemirel97@gmail.com

(1st International Conference on Engineering and Applied Natural Sciences ICEANS 2022, May 10-13, 2022)

(**DOI:** 10.31590/ejosat.1111208)

ATIF/REFERENCE: Demirel, M. (2022). Dual-band Band-pass Tunable Filter with Meander-Line Resonator. *European Journal of Science and Technology*, (36), 134-138.

Abstract

Radio frequency (RF) that can be tunable filters are band-pass filters (BPFs) with finely tunable passband frequencies. The passband frequency can be changed digitally, mechanically, or with a control voltage. Tunable BPF designs are increasing in importance as communication systems become more complex. In this study, a dual-band band-pass tunable filter with a meander-line resonator has been proposed. It aimed to create a tunable band-pass filter design in two different bands by using the SVM1413 varactor diode and gradually changing the capacitance value. SVM1413 varactor diode has been chosen in terms of applicability and capacitance value range width. The BPF operates in two different frequency ranges, from 2.5 to 3 GHz and from 4.2 to 4.6 GHz. BPF has been implemented and measured on a Rogers RO3003 substrate with a dielectric constant of 3 and a thickness of 1 mm. The substrate for the BPF has been chosen to be 30 × 30 mm^2 in size. The numerical calculation results have been simulated and optimized using computer simulation technology (CST). The insertion loss values are above -1 dB in both bandwidth ranges and all capacitance changes. Better results have been obtained when numerical calculation results have been compared with the outputs of the sources used.

Keywords: Band-pass filter, Compact filter design, Microstrip filter, Tunable, Varactor, Meander-line resonator, CST

Kıvrımlı Döngü Rezonatörlü Çift Bantlı Bant Geçiren Ayarlanabilir Filtre

Öz

Radyo frekanslarında (RF) kullanılabilen ayarlanabilir filtreler, ince ayarlanabilen geçiş bandı frekanslarına sahip bant geçiren filtrelerdir (BPF). Geçiş bandı frekansı dijital, mekanik veya bir control voltajı ile değiştirilebilir. İletişim sistemleri daha karmaşık hale geldikçe, ayarlanabilir BPF tasarımlarının önemi artmaktadır. Bu çalışmada, kıvrımlı döngü rezonatörlü çift bantlı bant geçiren ayarlanabilir bir filtre önerilmiştir. SVM1413 varaktör diyot kullanılarak ve kapasitans değeri kademeli olarak değiştirilerek iki farklı bantta ayarlanabilir bir bant geçiren filtre tasarımı oluşturulması amaçlanmıştır. Uygulanabilirlik ve kapasitans değer aralığı genişliği açısından SVM1413 varaktör diyot seçilmiştir. BPF, 2.5'den 3 GHz'e ve 4.2'den 4.6 GHz'e olmak üzere iki farklı frekans aralığında çalışır. BPF, dielektrik sabiti 3 alınarak 1 mm kalınlığa sahip bir Rogers RO3003 substratı üzerinde uygulanmış ve ölçülmüştür. BPF için alt tabaka 30 × 30 mm^2 boyutunda seçilmiştir. Sayısal hesaplama sonuçları, Computer Simulation Technology (CST) kullanılarak simüle edilmiş ve optimize edilmiştir. Ekleme kaybı değerleri hem bant genişliği aralığında hem de tüm kapasitans değişikliklerinde -1 dB'nin üzerindedir. Sayısal hesaplama sonuçları kullanılan kaynakların çıktıları ile karşılaştırıldığında daha iyi sonuçlar elde edilmiştir.

Anahtar Kelimeler: Band geçiren filtre, Kompakt filtre tasarımı, Mikroşerit filtre, Ayarlanabilir, Kıvrımlı döngü rezonatörü, CST

[*] Corresponding Author: mdemirel97@gmail.com

1. Introduction

Recently, wireless communication technologies have attracted alot of attention. As technology improves, communication systems have become more compact in comparison to conventional microwave/millimeter wave components [1-5]. Until now, various two-band and more-band BPFs have been proposed and demanded. Multiple resonators have required for multi-band filter designs. Due to the usage of a high number of resonators, the filter's size increases. In order to prevent this situation and provide high performance, microstrip filters have been recommended. Due to the freedom in design in microstrip filters, a suitable filter has been recommended by designing geometries specifically for different needs [6-12].

The internal capacitance of a varactor diode changes with the reverse voltage. It is a voltage-dependent semiconductor device that always runs in the reverse bias condition. Varactor diodes are widely used in microstrip filters to keep the frequency band constant, because the capacitance value is adjustable depending on the voltage and because of its miniature size [13], [14]. In [15], An adjustable BPF with compact size and frequency-invariant passband characteristics has been offered. The proposed BPF has been made adjustable between 1.7 and 2.1 GHz with 5% Chebyshev constant fractional bandwidth by controlling the DC bias voltage.

In [16], a BPF formed by a two varactor tuned switchable resonator with a continuous frequency tuning range that switchable to higher and lower resonance modes has been presented. Designed with microstrip technology, the BPF has a frequency tuning range of 1.1 to 2.1 GHz and a fixed absolute bandwidth of 40 MHz. In [17], a dual-band filter has been proposed, which can be switched from band-pass to band-stop filter by changing the state of the p-i-n diode. In [18], a compact third-order microstrip open-loop ring resonator tunable BPF has been offered to cover the 3.4 to 3.8 GHz frequency band for 5G applications.

In this study, a dual-band band-pass tunable filter with a meander-line resonator has been proposed. Simulation results have been obtained with CST software. BPF SMV1413 varactor diode has been adjusted to work in harmony with capacitance values. The BPF provided a wide tuning range to cover the frequency band from 2.6 GHz to 3 GHz and from 4.3 GHz to 4.6 GHz. The results have been analyzed and a complex and miniature BPF is proposed to work in concert with the SVM 1413 varactor diode.

2. Material and Method

In this section, the dual-band BPF design has been introduced. The geometry of the BPF has shown in Figure 2 and Figure 3. The size of the substrate used in the BPF has been chosen as $30 \times 30\ mm^2$. The proposed BPF has been placed on a normal 1 mm thick Rogers RO3003 substrate with a dielectric constant ε of 3. The ground has been covered the bottom of the filter completely. The BPF consists of four different resonator sections and has been powered by two ports with 50 Ω input impedance to eliminate the need for vias. Three of the resonators are open and one is closed as meander line resonator.

2.1. BPF Design and Performance

In this section, a deduced numerical calculation results have been obtained without using any device in BPF. According to the results, the BPF design has a good return loss (S_{11}) -30 dB at 3.55 GHz shown in Figure 1. The insertion value (S_{21}) is -0.3 dB at 3.55 GHz and bandwidth is between 3.40 and 3.70 GHz. In the next section, the design of the tunable BPF is discussed.

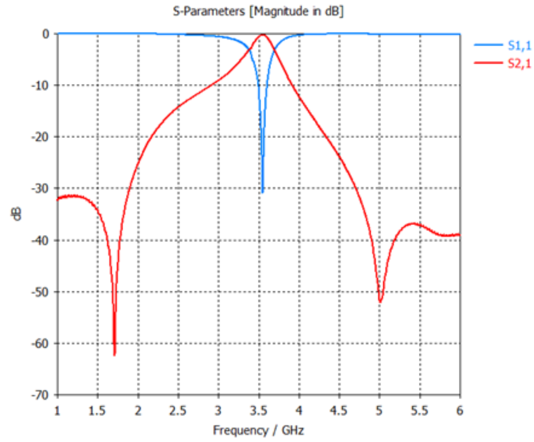

Fig. 1 Numerical Calculation Results

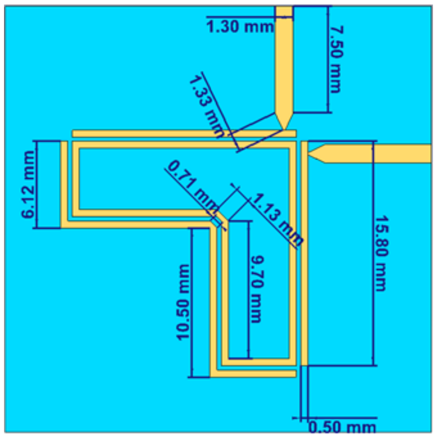

Fig. 2 BPF Design Top Side

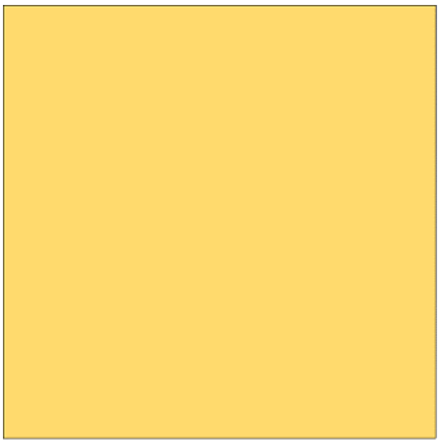

Fig. 3 BPF Design Bottom Side

2.2. Dual-band Tunable BPF Design and Performance

In this section, varactor diode added to the design and numerical calculation results have been obtained. The design has been adjusted for easy placement of the varactor diode. The dual-band tunable BPF design has been shown in Figure 4. As mentioned before, the SVM1413 varactor diode has been used in the study. The reason for choosing the SVM1413 is that the capacitance variation range is larger at different reverse voltage values applied. The change in capacitance values of about 8pF has resulted to further increase the adjustability range. The change in return loss and insertion loss values at different capacitance values has observed in four different figures. According to the results, it has been observed that insertion loss and return loss values at 2.5 to 3 GHz in Figure 5 and Figure 6, these values at 4.2 to 4.6 GHz in Figure 7 and Figure 8.

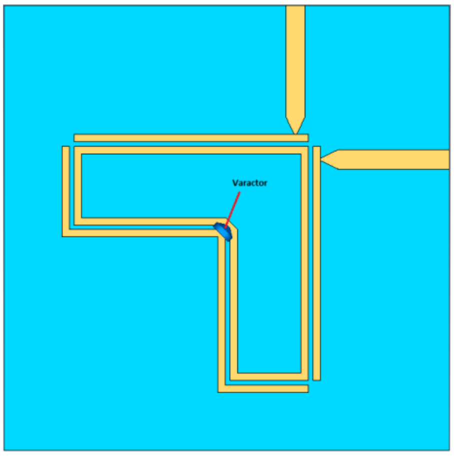

Fig. 4 Dual-band Tunable BPF Design

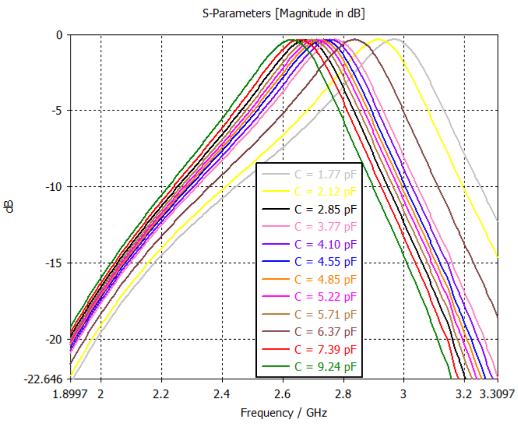

Fig. 5 Numerical calculation results of insertion loss (S_{21}) with different biasing voltages at 2.5 to 3 GHz

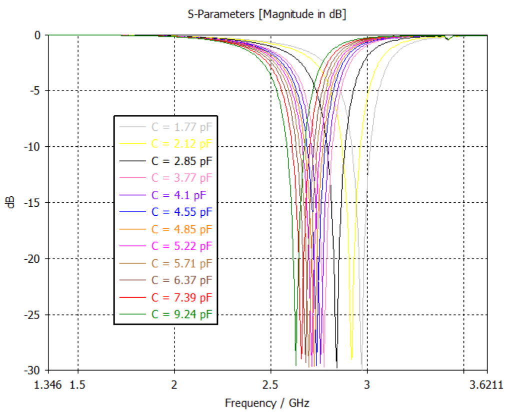

Fig. 6 Numerical calculation results of return loss (S_{11}) with different biasing voltages at 2.5 to 3 GHz

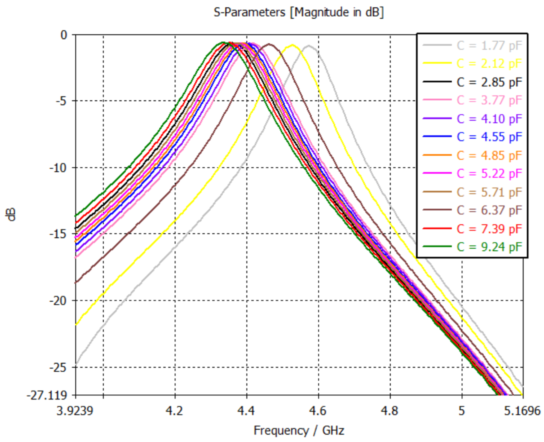

Fig. 7 Numerical calculation results of insertion loss (S_{21}) with different biasing voltages at 4.2 to 4.6 GHz

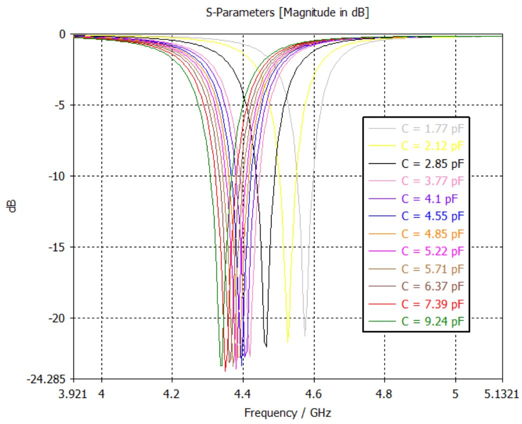

Fig. 8 Numerical calculation results of return loss (S_{11}) with different biasing voltages at 4.2 to 4.6 GHz

3. Results and Discussion

Table 1. Summary of numerical calculation result at 2.5 to 3 GHz

Reverse Voltage (V)	Varactor Capacitance (pF)	Resonant Frequency (GHz)	S_{11}(dB)	S_{21}(dB)
0	9.24	2.63	-29.6	-0.36
0.5	7.39	2.65	-28.9	-0.35
1	6.37	2.68	-29.3	-0.35
1.5	5.71	2.69	-29.7	-0.35
2	5.22	2.71	-29.7	-0.35
2.5	4.85	2.72	-29.6	-0.35
3	4.55	2.73	-29.6	-0.35
4	4.10	2.76	-29.4	-0.35
5	3.77	2.77	-29.7	-0.35
10	2.85	2.84	-29.8	-0.34
20	2.12	2.92	-29	-0.34
30	1.77	2.97	-29.9	-0.35

Table 2. Summary of numerical calculation result at 4.2 to 4.6 GHz

Reverse Voltage (V)	**Varactor Capacitance (pF)**	**Resonant Frequency GHz**	S_{11}**(dB)**	S_{21}**(dB)**
0	9.24	4.33	-23	-0.64
0.5	7.39	4.35	-23.7	-0.65
1	6.37	4.36	-23.2	-0.66
1.5	5.71	4.37	-23.3	-0.67
2	5.22	4.38	-23.6	-0.68
2.5	4.85	4.38	-23.3	-0.69
3	4.55	4.39	-22.7	-0.69
4	4.10	4.4	-22.7	-0.7
5	3.77	4.42	-22	-0.72
10	2.85	4.46	-22	-0.77
20	2.12	4.52	-21.7	-0.83
30	1.77	4.57	-21.3	-0.9

Since more than one change in capacitance has been observed, the results have been given in Table 1 and Table 2 in detail. Return loss values are below -20 dB in both frequency ranges. There is no loss in the insertion loss values from 2.5 to 3 GHz and the average value is -0.35 dB in all capacitance values change. Although there is a loss of -0.25 dB insertion loss in the range of 4.2 to 4.6 GHz, the insertion loss value has remained over -1 dB. Considering the bandwidth value at -10 dB return loss level, it is 50 MHz in the low GHz range and 100 MHz in the high GHz range. When the frequency level changes, the bandwidth value has remained constant and the return loss performance has preserved.

Since communication systems have formed by the combination of many systems, the proposed filters must work flexibly in certain frequency ranges. The reason for this is to prevent frequency deviations that may occur due to environmental factors and to stay in a more stable operating range. When the results have been analyzed, the proposed filter design has been worked without any performance loss in the determined frequency ranges.

4. Conclusions and Recommendations

This study has been explained in two different stages. In the first stage, a BPF design using a meander line resonator has been proposed. Good return loss and insertion loss values have been taken at 3.5 GHz level. In the second stage, a dual-band tunable filter design has been proposed using the same BPF topology and incorporating the SVM1413 varactor diode. As a result, of numerical computations, return loss and insertion loss values in two different bandwidths have good. The numerical simulations have produced better outcomes than the traditional techniques of design.

References

[1] Montero-de-Paz, J., Oprea, I., Rymanov, V., Babiel, S., García-Muñoz, L. E., Lisauskas, A., ... & Carpintero, G. (2013). Compact modules for wireless communication systems in the E-band (71–76 GHz). Journal of Infrared, Millimeter, and Terahertz Waves, 34(3), 251-266.

[2] Ozkaya, U., & Seyfi, L. (2015). Dimension optimization of microstrip patch antenna in X/Ku band via artificial neural network. Procedia-Social and Behavioral Sciences, 195, 2520-2526.

[3] Palandöken, M., Rymanov, V., Stöhr, A., & Tekin, T. (2012, August). Compact metamaterial-based bias tee design for 1.55 μm waveguide-photodiode based 71–76GHz wireless transmitter. In Progress in Electromagnetics Research Symposium, PIERS.

[4] Palandöken, M., & Sondas, A. (2014). Compact Metamaterial Based Bandstop Filter. Microwave Journal, 57(10).

[5] Palandoken, M. (2012). Metamaterial-based compact filter design. In Metamaterial. IntechOpen.

[6] Al-Yasir, Y. I., OjaroudiParchin, N., Abdulkhaleq, A., Hameed, K., Al-Sadoon, M., & Abd-Alhameed, R. (2019, July). Design, simulation and implementation of very compact dual-band microstrip bandpass filter for 4G and 5G applications. In 2019 16th international conference on synthesis, modeling, analysis and simulation methods and applications to circuit design (SMACD) (pp. 41-44). IEEE.

[7] Afzali, B., Abbasi, H., Shama, F., & Dehdasht-Heydari, R. (2021). A microstrip bandpass filter with deep rejection and low insertion loss for application at 2.4 GHz useful wireless frequency. AEU-International Journal of Electronics and Communications, 138, 153811.

[8] Palandoken, M., and H. Henke. "Fractal spiral resonator as magnetic metamaterial." 2009 Applied Electromagnetics Conference (AEMC). IEEE, 2009.

[9] Ieu, W., Zhang, D., Lv, D., & Wu, Y. (2018). Dual-band microstrip bandpass filter with independently-tunable passbands using patch resonator. Electronics Letters, 54(10), 665-667.

[10] Karthie, S., & Salivahanan, S. (2019). Fractally slotted patch resonator based compact dual-mode microstrip bandpass filter for Wireless LAN applications. AEU-International Journal of Electronics and Communications, 107, 264-274.

[11] Nieto, J., & Sauleau, R. (2006, November). Miniature coplanar waveguide and microstrip stop-band filters using spiral resonators. In 2006 First European Conference on Antennas and Propagation (pp. 1-5). IEEE.

[12] Al-Nuaimi, M. K. T., & Whittow, W. G. (2010, April). Compact microstrip band stop filter using SRR and CSSR: Design, simulation and results. In Proceedings of the Fourth European Conference on Antennas and Propagation (pp. 1-5). IEEE.

[13] Tang, W., & Hong, J. S. (2010). Varactor-tuned dual-mode bandpass filters. IEEE Transactions on Microwave Theory and Techniques, 58(8), 2213-2219.

[14] Long, J., Li, C., Cui, W., Huangfu, J., & Ran, L. (2011). A tunable microstrip bandpass filter with two independently adjustable transmission zeros. IEEE Microwave and Wireless Components Letters, 21(2), 74-76.

[15] Tsai, H. Y., Huang, T. Y., & Wu, R. B. (2016). Varactor-tuned compact dual-mode tunable filter with constant passband characteristics. IEEE Transactions on Components, Packaging and Manufacturing Technology, 6(9), 1399-1407.

[16] Chen, C. F., Wang, G. Y., & Li, J. J. (2018). Microstrip switchable and fully tunable bandpass filter with continuous frequency tuning range. IEEE Microwave and Wireless Components Letters, 28(6), 500-502.

[17] Chen, F. C., Li, R. S., & Chen, J. P. (2018). A tunable dual-band bandpass-to-bandstop filter using pin diodes and varactors. IEEE Access, 6, 46058-46065.

[18] Al-Yasir, Y. I., Parchin, N. O., Alabdallah, A., Abdulkhaleq, A. M., Abd-Alhameed, R. A., & Noras, J. M. (2019,

September). Design of bandpass tunable filter for green flexible RF for 5G. In 2019 IEEE 2nd 5G World Forum (5GWF) (pp. 194-198). IEEE.